

Supplementary Information

Metal-Free Polymer Photocatalysts for Efficient Gas-Phase Reduction of Atmospheric CO₂ and Simultaneous H₂O₂ Production

Wei Wu,^{†§} Mantao Chen,^{†§} Chunyuan Feng,[#] Waner Li,[†] Tingting Zhang,[†] Chao Zeng,[‡] Bo Wang,[†] Lixiang Zhong^{#*} and Chunhui Dai^{†*}

[†]Jiangxi Key Laboratory for Mass Spectrometry and Instrumentation, School of Chemistry and Materials Science, East China University of Technology, Nanchang 330013, P. R. China.

[#]Centre for Quantum Physics, Key Laboratory of Advanced Optoelectronic Quantum Architecture and Measurement (MOE), School of Physics, Beijing Institute of Technology, Beijing 100081, China.

[‡]School of Chemical Engineering, Jiangxi Normal University, Nanchang 330022, P. R. China.

[§]Both authors contribute equally

Corresponding Authors

*E-mail: zhonglx@bit.edu.cn; chunh-dai@ecut.edu.cn.

1. Experimental Section

Materials.

2,5-Diamino-1,4-benzenedithiol dihydrochloride (98% purity), tris(4-formylphenyl)amine (98% purity), 1,3,5-tris(4-formylphenyl)benzene (97% purity) and 4,4',4''-(1,3,5-triazine-2,4,6-triyl)tribenzaldehyde (97% purity) were supplied by Energy Chemical Co., Ltd (China). All these materials were used directly without further purification. Simulated flue gas (15% CO₂ and 85% N₂) was purchased from Nanchang grand gas Co., Ltd.

Synthesis of the polymers.

TPA-BBT was synthesized according to the reported method.¹ Tris(4-formylphenyl)amine (164.7 mg, 0.5 mmol) and 2,5-diamino-1,4-benzenedithiol dihydrochloride (245.2 mg, 1.0 mmol) were added in a 50 mL dry Schleck tube. 15 mL of DMF was then added to the tube and the reaction mixture was heated at 130 °C for 48 h. After cooling to room temperature, the precipitate was collected by centrifugation and washed with CH₂Cl₂, MeOH, DMF and water. The products were further purified by Soxhlet extraction with CH₂Cl₂ and then dried to give TPA-BBT as a bright yellow powder (281.1 mg, yield 86%). Anal. Calcd for (C₄₂H₂₁N₇S₆)_n: C, 61.82; H, 2.59; N, 12.02; S, 23.57; Found C, 67.13; H, 1.04; N, 10.98; S, 25.86%.

Synthesis of TPB-BBT. TPB-BBT was synthesized following the procedure described above for TPA-BBT from 1,3,5-tris(4-formylphenyl)benzene (195.2 mg, 0.5 mmol) and 2,5-diamino-1,4-benzenedithiol dihydrochloride (245.2 mg, 1.0 mmol). After drying, the final product TPB-BBT was obtained as a yellow-green yellow solid (296.7 mg, yield 83%). Anal. Calcd for (C₄₈H₂₄N₆S₆)_n: C, 65.73; H, 2.76; N, 9.58; S, 21.93; Found C, 61.46; H, 2.23; N, 10.14; S, 23.17%.

Synthesis of TPT-BBT. TPT-BBT was synthesized following the procedure described above for TPA-BBT from 2,4,6-tris(4-formylphenyl)-1,3,5-triazine (196.7 mg, 0.5 mmol) and 2,5-diamino-1,4-benzenedithiol dihydrochloride (245.2 mg, 1.0 mmol). After drying, the final product TPT-BBT was obtained as a yellow solid (312.3 mg, yield 87%). Anal. Calcd for $(C_{45}H_{21}N_9S_6)_n$: C, 61.41; H, 2.41; N, 14.32; S, 21.86; Found C, 58.05; H, 3.19; N, 15.67; S, 23.21%.

Material characterizations.

The ^{13}C CP/MAS NMR spectra of the polymers was recorded on a Bruker Avance III 400 spectrometer. Fourier transform infrared (FTIR) spectra of the samples were performed on a Nicolet-iS10 FTIR spectrometer (Thermo Scientific, USA) in the range 4000-400 cm^{-1} . C, H, N and S elemental analysis of the polymers were performed on a Elementar vario MICRO cube. The morphologies of the as-synthesized polymers were characterized by SEM (Zeiss Gemini 300, Germany). The powder X-ray diffraction (PXRD) patterns were obtained using a Bruker D8 X Ray Diffractometer. Thermogravimetric analysis (TGA) was inspected using a Netzsch TG209F1 with an automated vertical overhead thermobalance under nitrogen flow, ramping heating at 10 $^{\circ}C\ min^{-1}$ from 50 $^{\circ}C$ to 800 $^{\circ}C$. The porosity properties were derived from N_2 adsorption-desorption isotherms at 77 K using a Micromeritics ASAP 2460 volumetric adsorption analyzer. The samples were degassed in vacuum at 100 $^{\circ}C$ for 10 h, and then measured at 77 K and 273/298 K to determine N_2 and CO_2 adsorption, respectively. The CO_2 uptake capacities of the polymer at 273 and 298 K make it facile to compare the adsorption performance with other reported polymer adsorbents.¹⁻³ Based on the ambient conditions for photocatalytic reaction in this study, the CO_2 uptake of the polymer at 298 K and atmospheric pressure is important to reveal the selective CO_2 capture of polymer photocatalyst over N_2 during photocatalysis. Therefore, the CO_2 uptake of polymer photocatalysts at high temperature and

pressure haven't been explored. UV vis diffuse reflectance spectra (DRS) were measured by a Shimadzu UV 3600 spectrometer equipped with an integrating sphere and BaSO₄ was used as a reference. Photoluminescence (PL) spectra were recorded by an Edinburgh FLS980 coupled with a time correlated single photo counting system at room temperature.

Photocatalytic CO₂ reduction with water vapor

The photocatalytic tests of the polymers were carried out in a 160 mL custom-made glass reactor with a quartz glass cap under ambient conditions. A 300 W Xe arc lamp with a AM1.5 filter was used to provide the simulated solar light (100 mW/cm²). In a typical experiment, 20 mg of ground polymer powders was deposited on a glass slide with a fixed area of 9 cm² and then the glass slide was put on a sample holder in the reactor. Before the irradiation, 5 mL of water was added at the bottom of the reactor to generate water vapor. The gas products during photocatalytic process was analyzed at an interval of 1h by a gas chromatography equipped with an FID and a TCD detector (A60, PANNA, China). Meanwhile, 0.5 mL of liquid samples were withdrawn from the bottom of reactor for the detection of produced H₂O₂ according to the reaction: $\text{H}_2\text{O}_2 + 3\text{I}^- + 2\text{H}^+ \rightarrow \text{I}_3^- + 2\text{H}_2\text{O}$. An equal volume of potassium diphthalate (0.1 M, 1 mL) and KI (0.4 M, 1 mL) solution were added into the solution. After 15 min in the dark, the absorbance of I₃⁻ at 350 nm was measured by UV-1900i spectrophotometer (Shimadzu). Control tests were performed in the absence of water vapor, CO₂, polymer photocatalysts or light irradiation. Isotopic experiments were conducted using ¹³CO₂, O₂ and H₂O¹⁸, and NaOH aqueous solution (2 M) were added to consume unreacted ¹³CO₂ in the reactor after photocatalytic reaction. The generated CO, H₂O₂ and O₂ was analyzed by gas chromatography mass spectrometry (GC-MS).

Photoelectrochemical properties measurements

Electrochemical measurements were performed by an electrochemical analyzer (CHI 660E, Chenhua, China) with a standard three-electrode cell at room temperature. The polymer sample, an Ag/AgCl electrode (saturated KCl), and a Pt wire are used as the working electrode, the reference electrode, and the counter electrode, respectively. The polymer sample was casted on the surface of a fluorine-doped tin oxide (FTO) glass and dried in air. Na₂SO₄ aqueous solution (1 M, pH = 7) was used as the electrolyte and a bias voltage of +0.6 V was used in the measurement. A 300 W Xenon lamp was used as the light source, while EIS plots were obtained in the dark. The EIS spectra were recorded by applying a 10 mV AC signal in the frequency range from 100 kHz to 0.01 Hz with the initial potential (+0.6 V).

Electrochemical measurements

Electrochemical properties of the polymers were tested in a deoxygenated anhydrous acetonitrile solution containing 0.1 M tetrabutylammonium hexafluorophosphate (Bu₄NPF₆) as an electrolyte. The Pt wire, sample coated glassy carbon electrode, and Ag/AgNO₃ electrode (in acetonitrile solution containing 0.1 M Bu₄NPF₆ and 0.01 M AgNO₃) were used as the working electrode, counter electrode, and reference electrode in the electrochemical analyzer system. The potential was recorded against ferrocene/ferrocenium (Fc/Fc⁺). For the conversion from the Fc/Fc⁺ redox couple to the normal hydrogen electrode (NHE), the equation $E_{\text{NHE}} = E_{\text{Fc/Fc}^+} + 0.63 \text{ V}$ was applied.

DFT Calculations

First-principles calculations were carried out using density functional theory (DFT) method as implemented in the Vienna ab initio simulation package (VASP).⁴ The ion-electron interactions were treated with the projected augmented wave pseudopotentials,⁵ and the general gradient approximation (GGA) with the Perdew-Burke-Ernzerhof functional was used to describe the exchange-correlation potential when performing geometric relaxations.⁶ Hybrid functional of Heyd, Scuseria, and Ernzerhof (HSE06) were used for electronic structures calculations.⁷ The plane-wave basis was expanded up to a cutoff energy of 400 eV, which is the highest recommended cutoff energy of elements involved in this work, i.e., H, C, N, O, and S. All structures were relaxed using a conjugate gradient method until the residual force on every atom was less than 0.02 eV/Å, and the convergence criteria of total energy in the self-consistent field method was set to 10⁻⁵ eV.

2. Results.

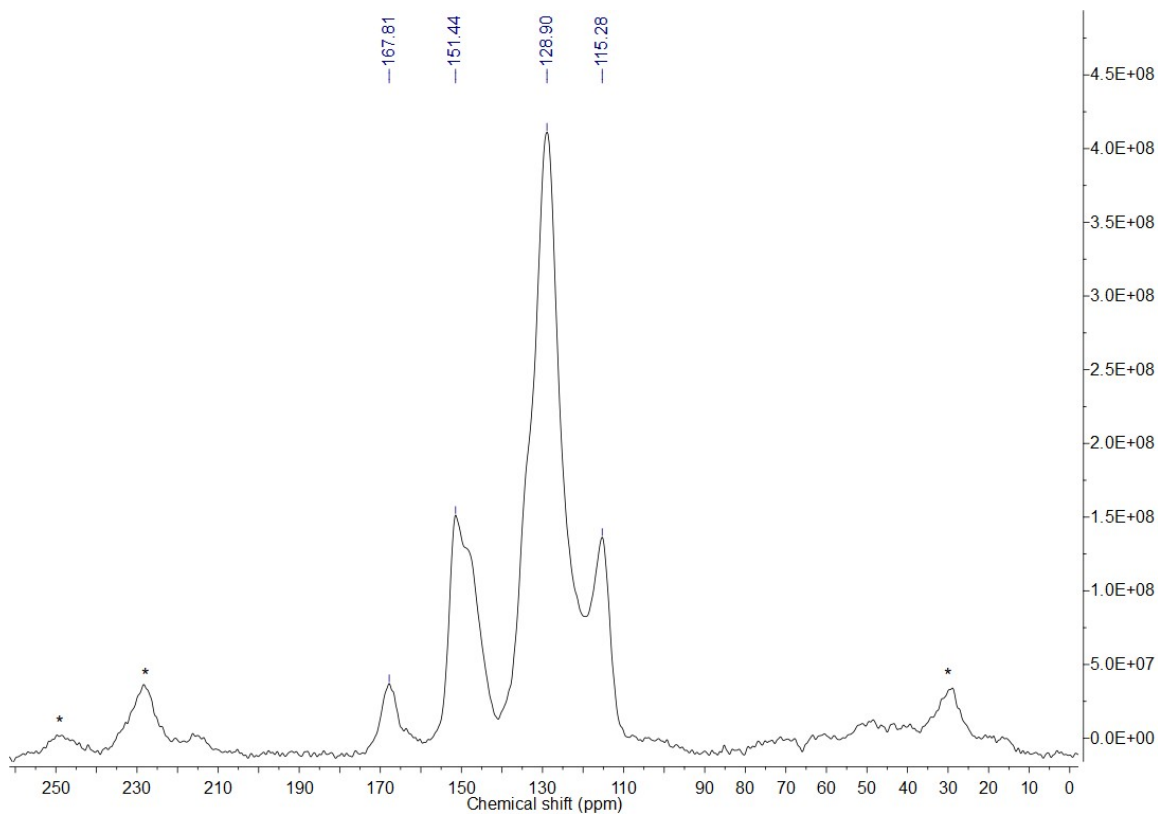


Figure S1. Solid-state ¹³C CP/MAS NMR spectrum of TPA-BBT.

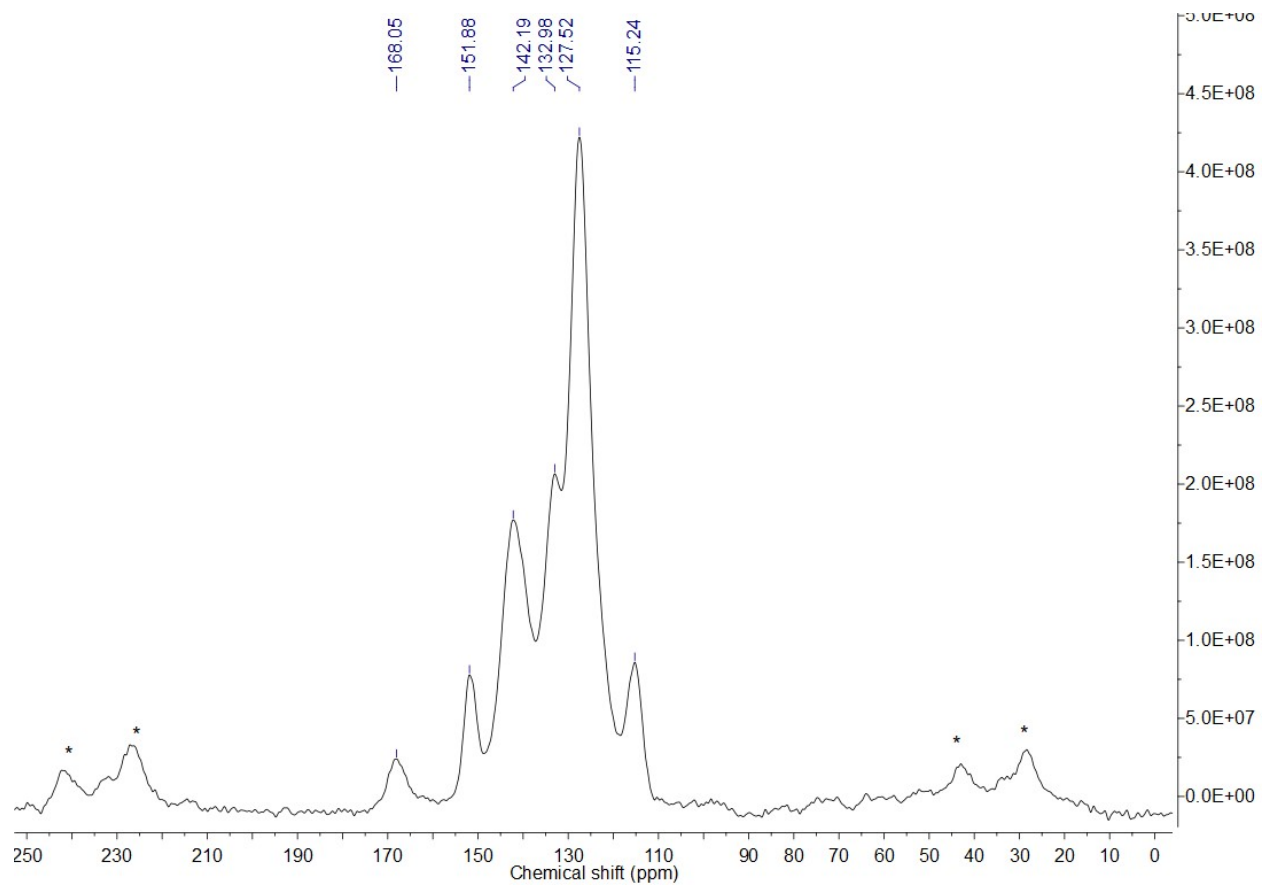


Figure S2. Solid-state ^{13}C CP/MAS NMR spectrum of TPB-BBT.

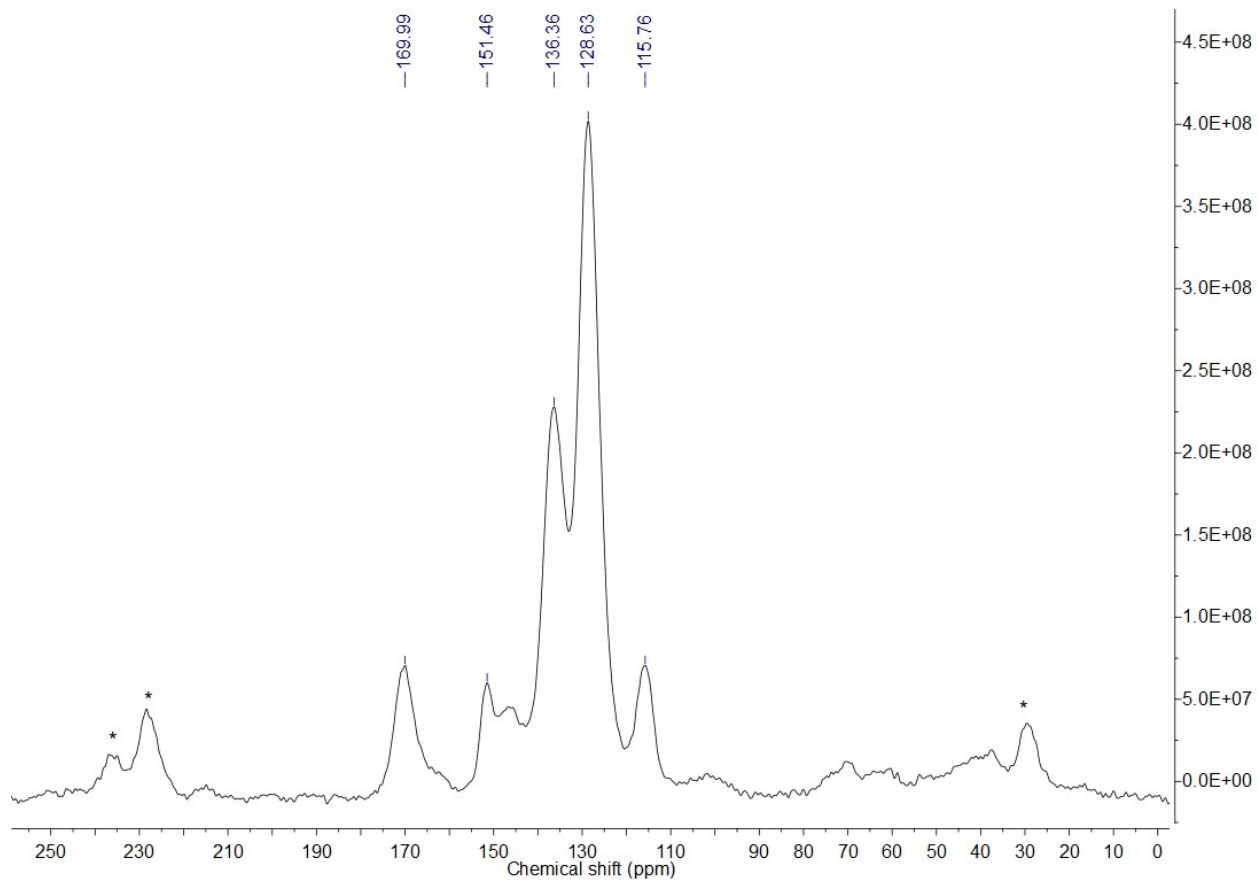


Figure S3. Solid-state ^{13}C CP/MAS NMR spectrum of TPT-BBT.

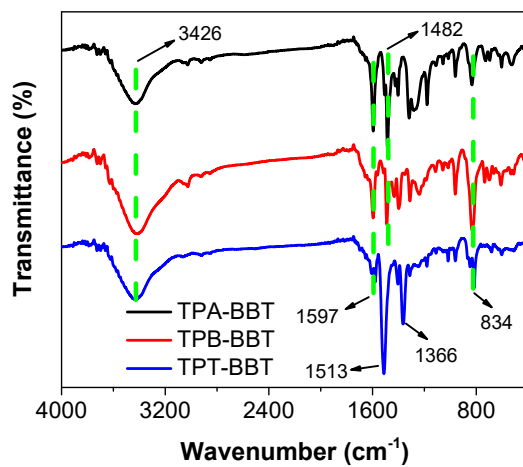


Figure S4. FT-IR spectra of the polymers.

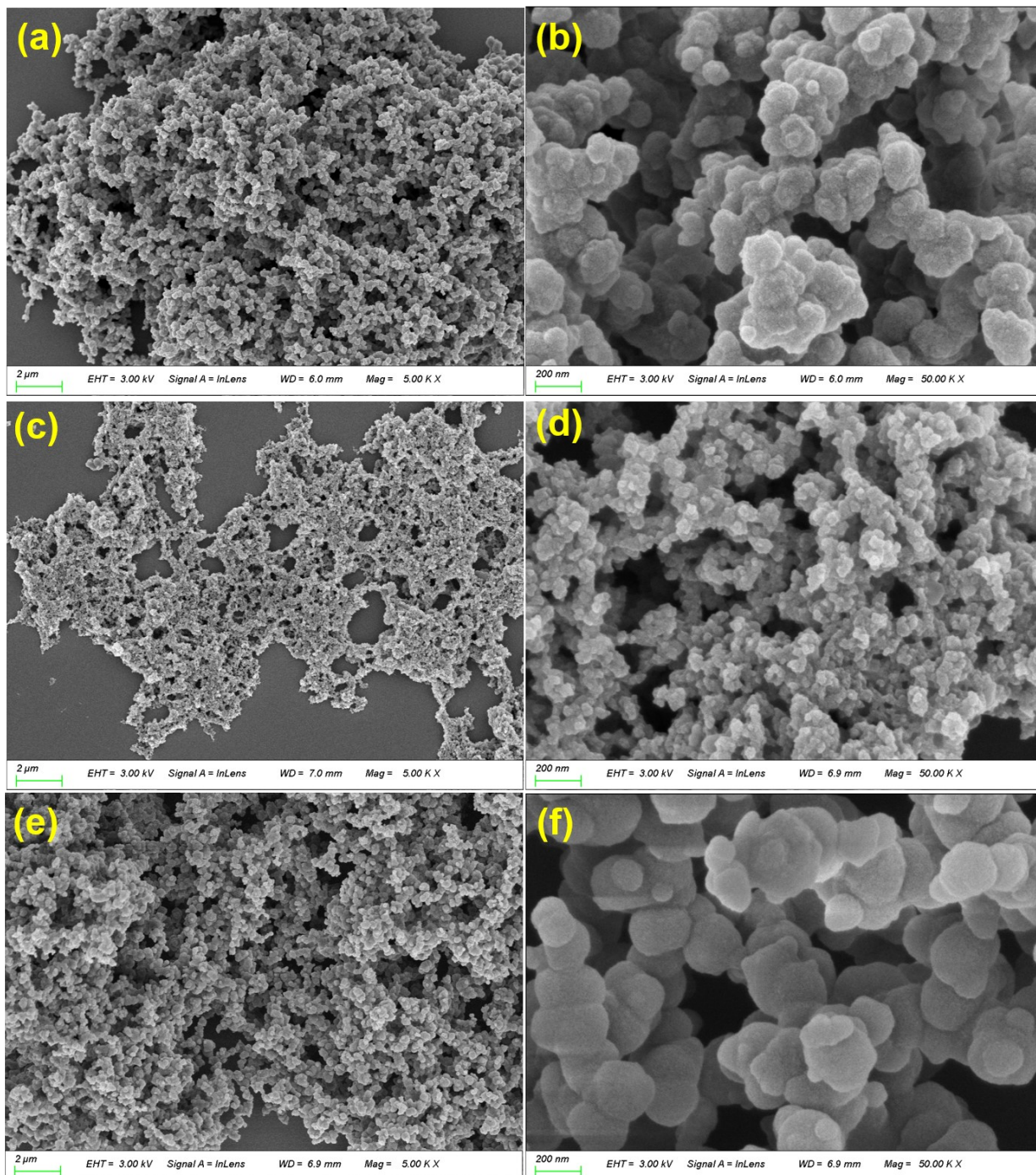


Figure S5. SEM images of TPA-BBT (a,b), TPB-BBT (c,d) and TPT-BBT (e,f).

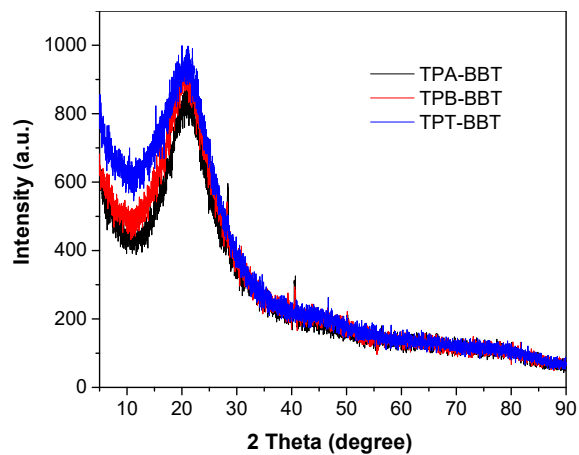


Figure S6. PXRD patterns of the polymers.

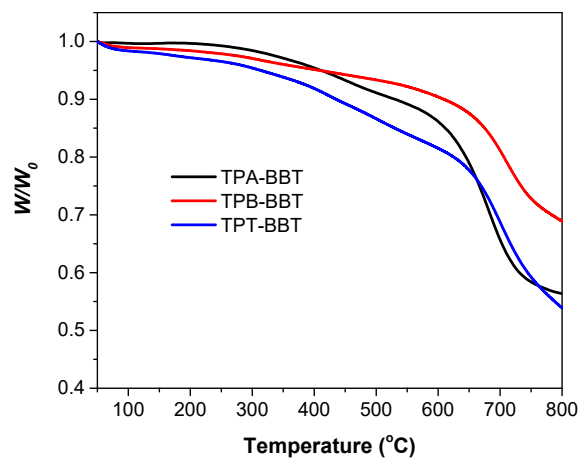


Figure S7. Thermogravimetric analysis (TGA) curves of the polymers.

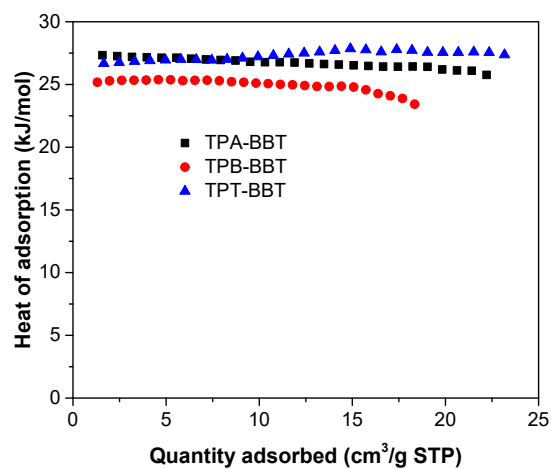


Figure S8. The calculated isosteric heat (Q_{st}) of CO_2 adsorption on the polymers at different CO_2 loadings.

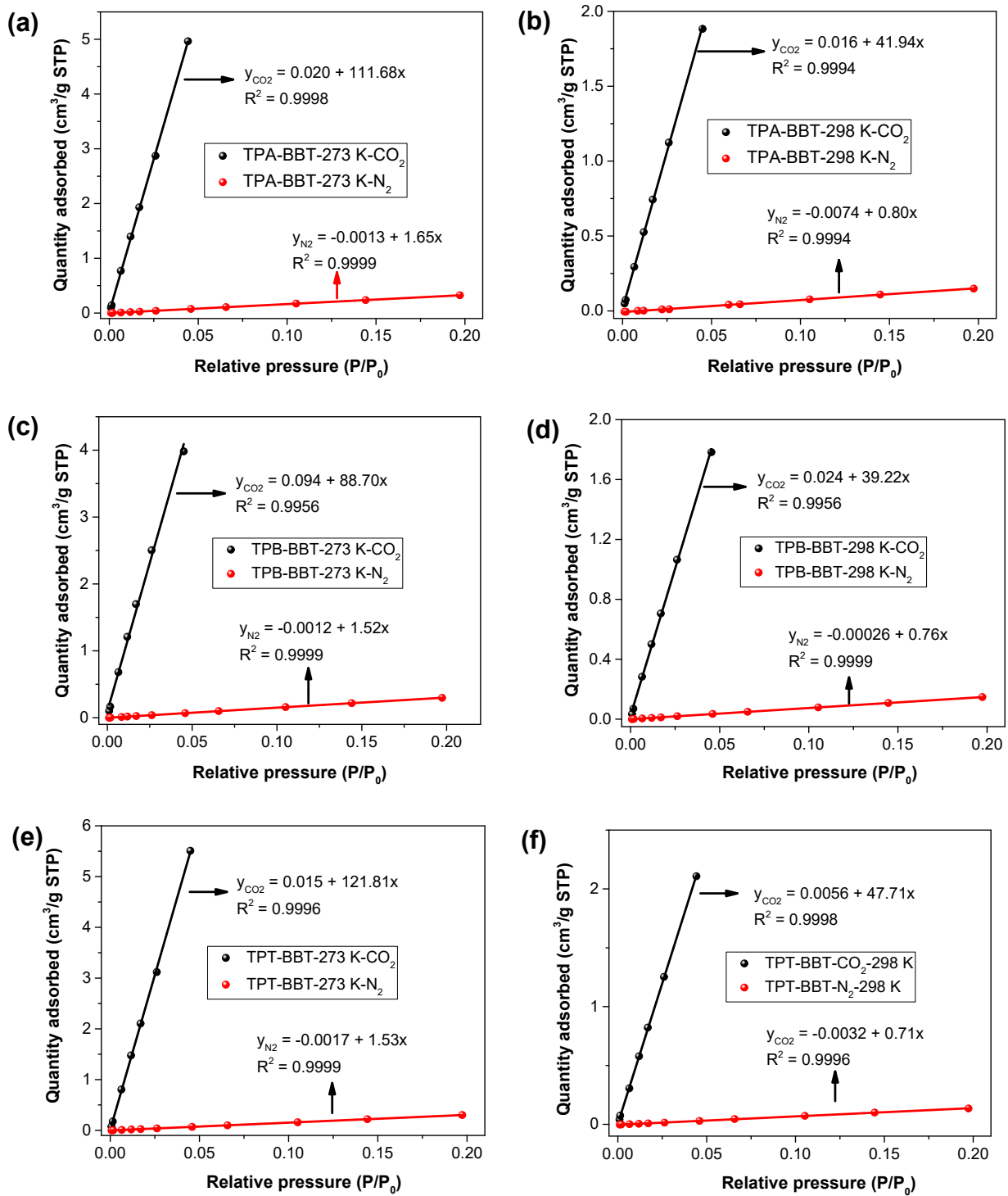


Figure S9. The selectivity of polymers for CO₂ over N₂ isotherms obtained from the initial slope method.

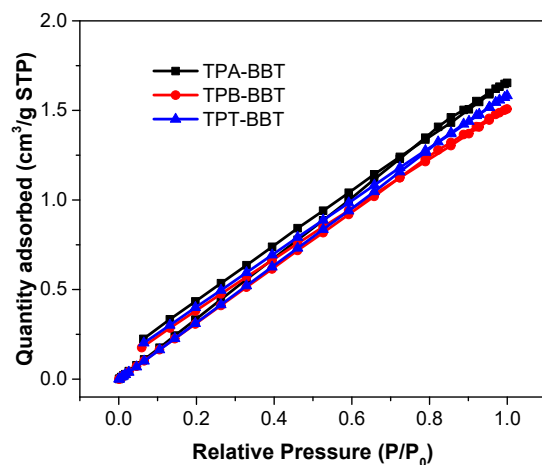


Figure S10. The O_2 adsorption of the polymers at 298 K.

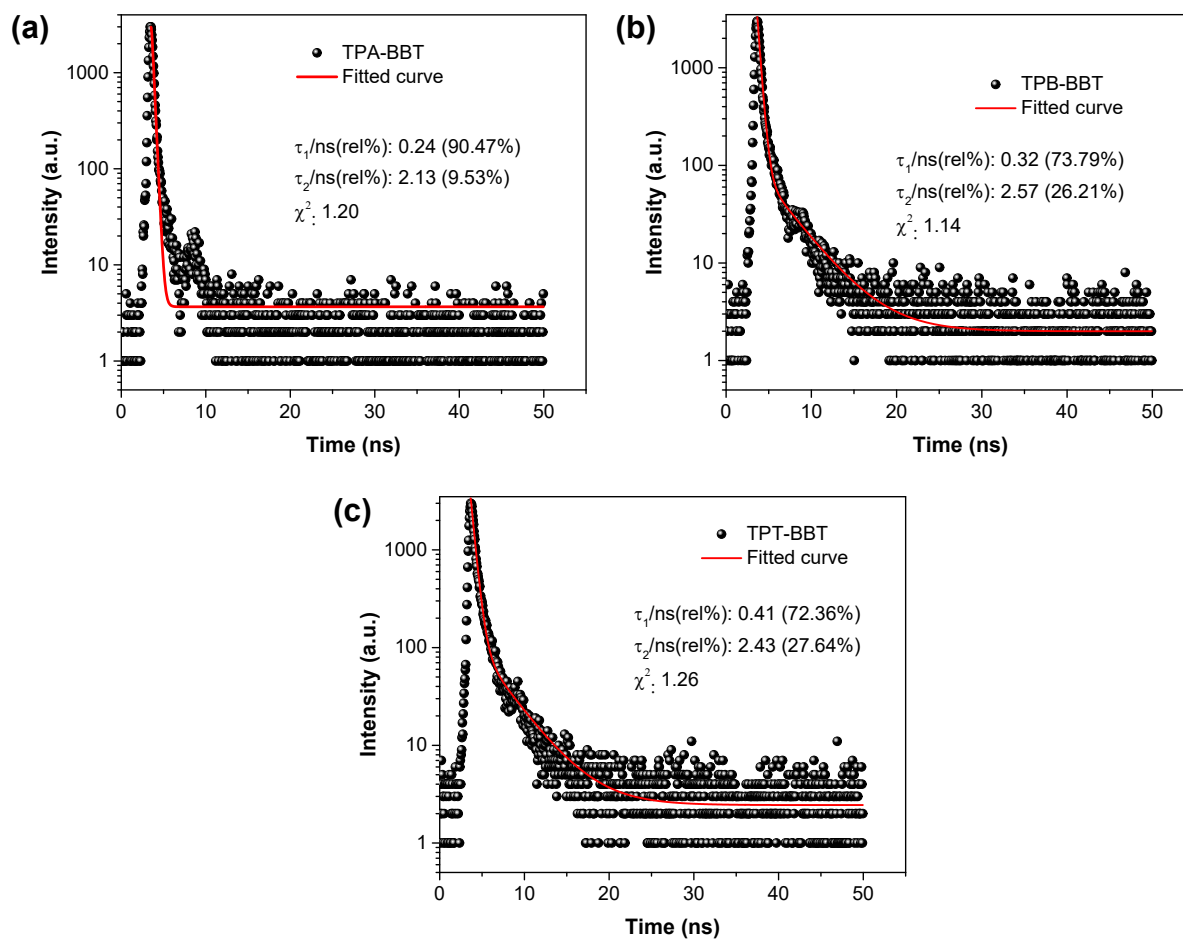


Figure S11. The photoluminescence decay parameters of the polymer powders fitted curves by bi-exponential decay equation.

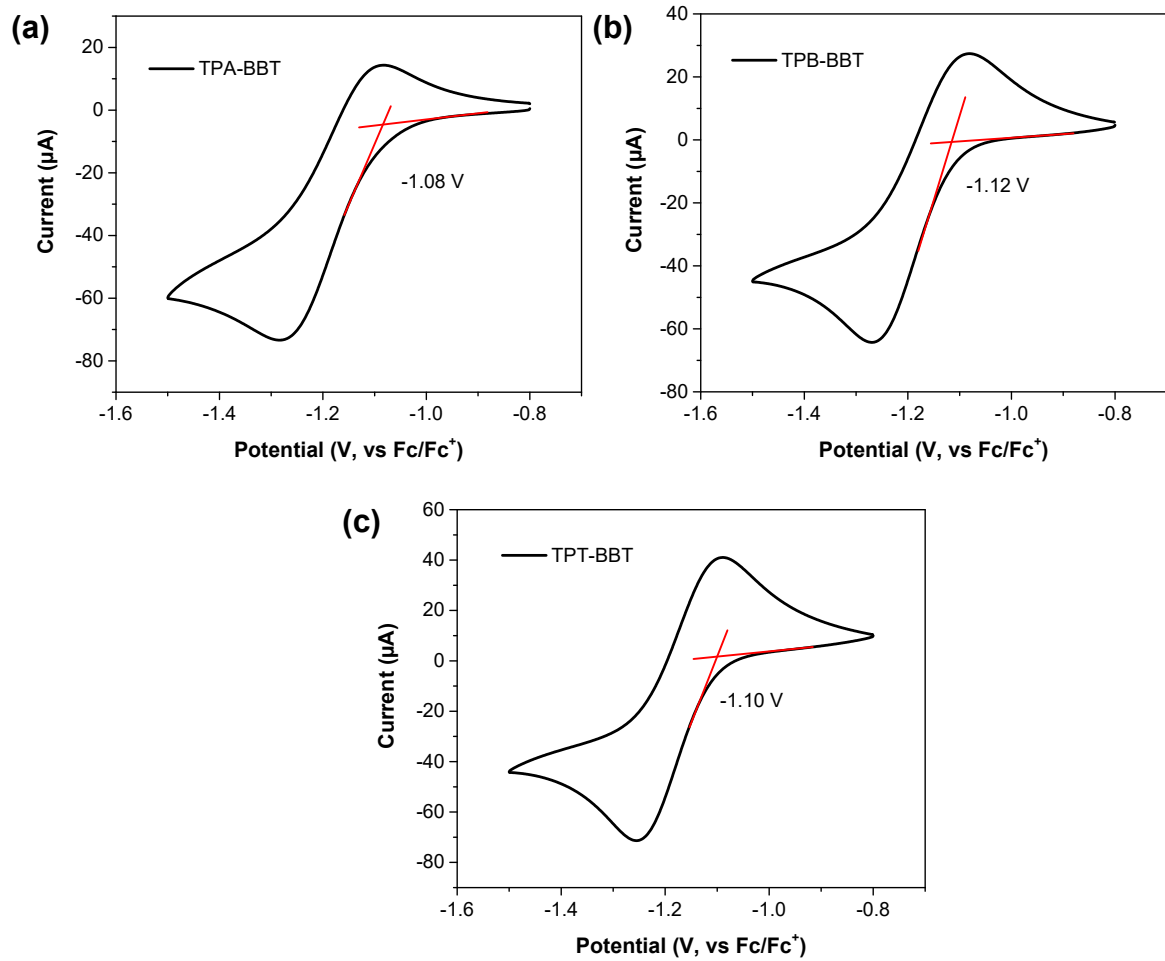


Figure S12. Reduction cyclic voltammetric waves of polymer modified glassy carbon electrode (vs Ag/Ag^+ in acetonitrile solution with 0.1 M $n\text{-Bu}_4\text{NPF}_6$ as supporting electrolyte).

Table S1. Photocatalytic activity of CO₂ reduction coupled H₂O₂ production in recent reports.

Light source	Photocatalytic materials	Main products and highest efficiency	Reference
100 W high-pressure mercury lamp	Ag–MnOx/CaTiO ₃	CO: ~42 μmol h ⁻¹ g ⁻¹ H ₂ O ₂ : ~48 μmol h ⁻¹ g ⁻¹	<i>ACS Appl. Energy Mater.</i> 2021 , 4, 6500.
300 W Xe lamp	D-A conjugated polymers	CH ₄ : 10.6 μmol h ⁻¹ g ⁻¹ H ₂ O ₂ : 350 μmol h ⁻¹ g ⁻¹	<i>Angew. Chem. Int. Ed.</i> 2023 , 62, e202313392.
300 W Xe lamp	NH ₂ -MIL-125-Ti/WO _{3-x}	CO: 12.57 μmol h ⁻¹ g ⁻¹ H ₂ O ₂ : 8.41 μmol h ⁻¹ g ⁻¹	<i>Chem. Eng. J.</i> 2023 , 466, 143129.
300 W Xe lamp	Sb-alloyed Cs ₄ MnBi ₂ Cl ₁₂ perovskites	CO: 35.1 μmol h ⁻¹ g ⁻¹ H ₂ O ₂ : 15.68 μmol h ⁻¹ g ⁻¹	<i>J. Energy Chem.</i> 2023 , 82, 18.
300 W Xe lamp	Ag(I) clusters/Fe(II) porphyrinates/metal-organic frameworks	CO: 36.5 μmol h ⁻¹ g ⁻¹ H ₂ O ₂ : 35.9 μmol h ⁻¹ g ⁻¹	<i>Angew. Chem. Int. Ed.</i> 2024 , e202412553, https://doi.org/10.1002/anie.202412553

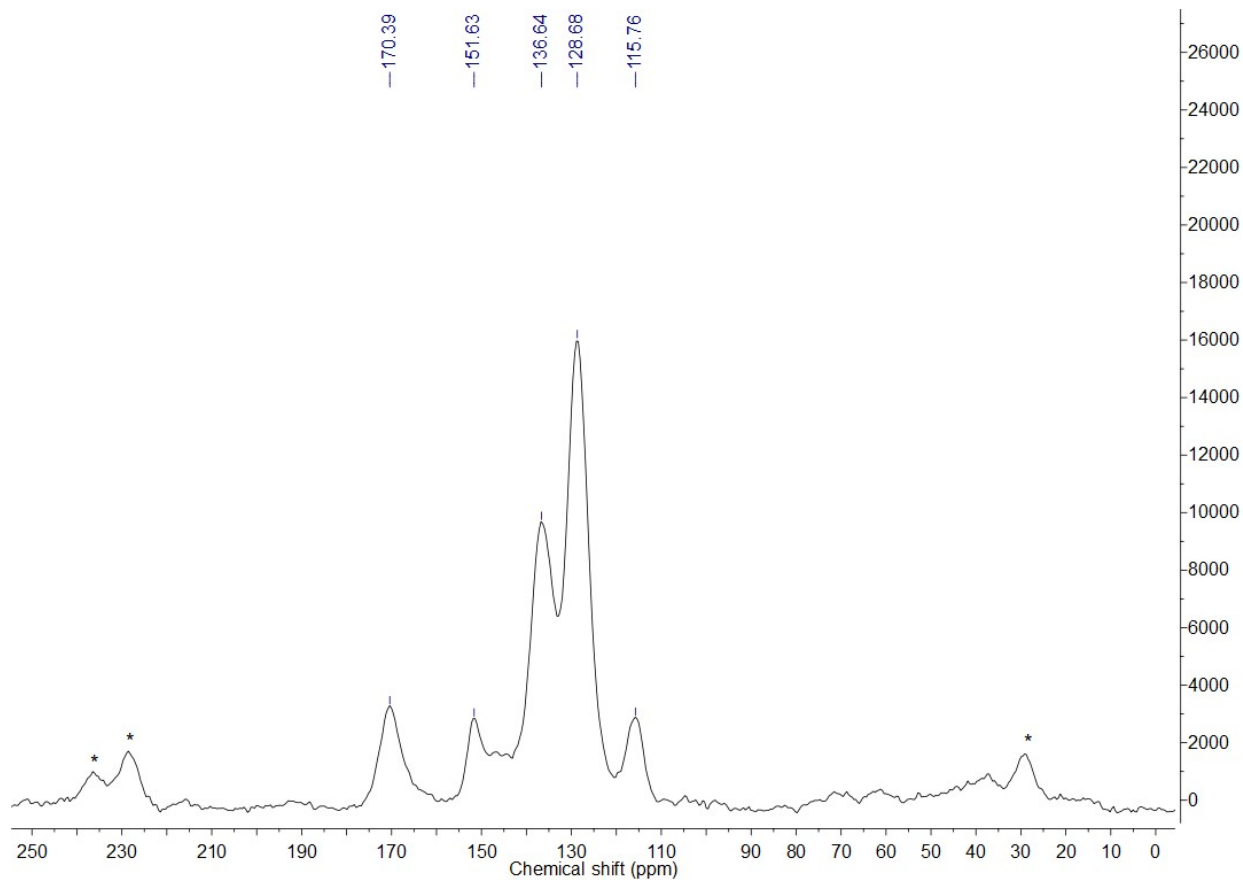


Figure S13. CP MAS ^{13}C NMR spectrum of TPT-BBT after the cyclic test.

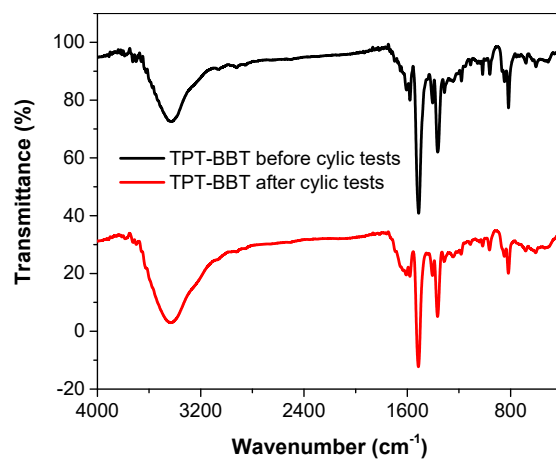


Figure S14. FT-IR spectrum of TPT-BBT after the cyclic test.

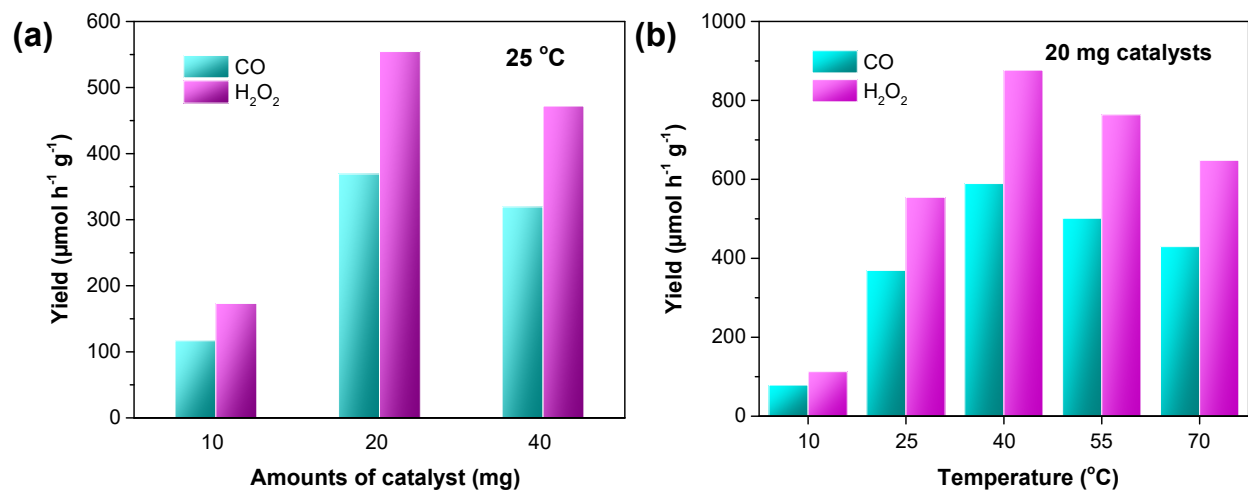


Figure S15. The photocatalytic performances of TPT-BBT in air under different conditions (a) different amounts of catalyst and (b) temperatures.



Figure S16. The gas-phase CO₂ photoreduction experiment over TPT-BBT at East China University of Technology (Nanchang campus, China) on Aug 6th, 2024. Reaction time: from 13:00 pm to 16:00 pm, solar intensity: $\sim 72.5 \text{ mW/cm}^2$, outdoor temperature: 41 °C at 13:00 pm.

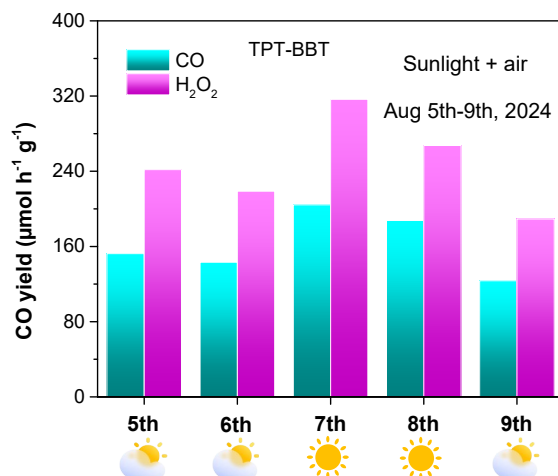


Figure S17. The average CO and H₂O₂ yield TPT-BBT under natural sunlight irradiation (from 13:00 pm to 16:00 pm) and air atmosphere on Aug 5th-9th, 2024.

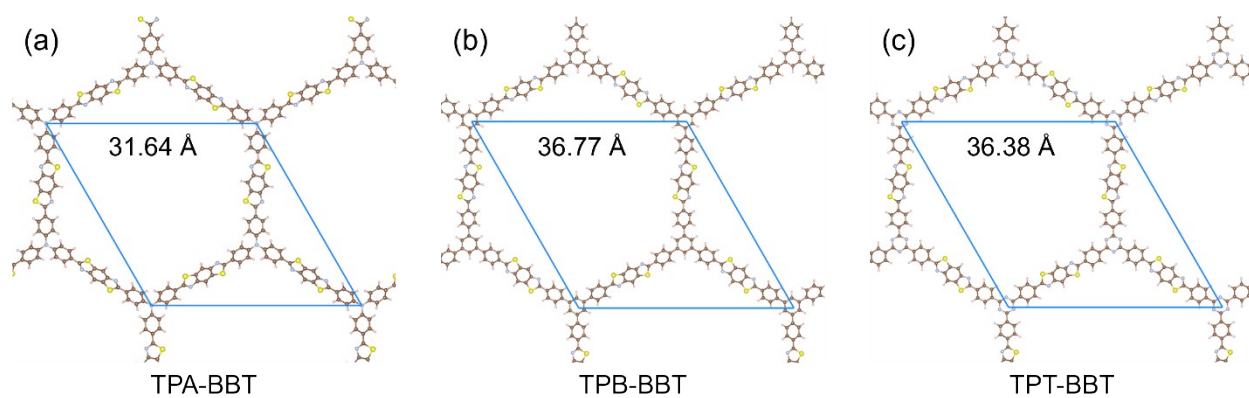


Figure S18. Optimized model structures of TPA-BBT (a), TPB-BBT (b) and TPT-BBT (c) in DFT calculations.

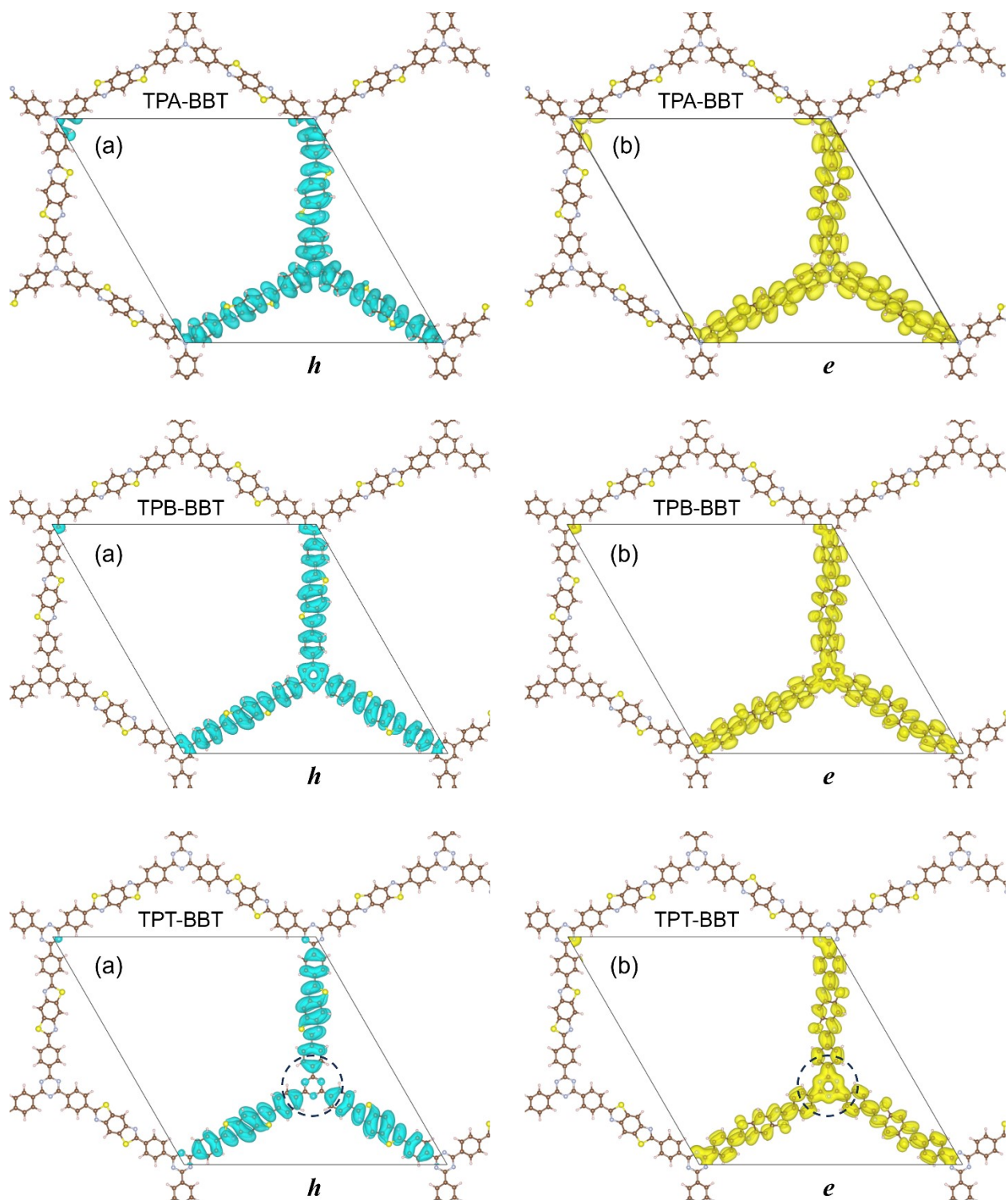


Figure S19. Excited-state hole distribution (a) and electron distribution (b) for the polymers ($0.0002 \text{ e bohr}^{-3}$).

References:

- [1] K. S. Song, P. W. Fritz, A. Coskun, *Chem. Soc. Rev.* **2022**, *51*, 9831.
- [2] M. S. Khosrowshahi, H. Mashhadimoslem, H. Shayesteh, G. Singh, E. Khakpour, X. Guan, M. Rahimi, F. Maleki, P. Kumar, A. Vinu, *Adv. Sci.* **2023**, *10*, 2304289.
- [3] D. Barker-Rothschild, J. Chen, Z. Wan, S. Renneckar, I. Burgert, Y. Ding, Y. Lu, O. J. Rojas, *Chem. Soc. Rev.* **2025**, *54*, 623.
- [4] R. Anbazhagan, R. Krishnamoorthi, D. Thankachan, T. T. V. Dinh, C.-F. Wang, J. M. Yang, Y.-H. Chang, H.-C. Tsai, *Langmuir* **2022**, *38*, 4310.
- [5] G. Kresse, J. Furthmüller, *Phys. Rev. B* **1996**, *54*, 11169.
- [6] P. E. Blochl, *Phys. Rev. B* **1994**, *50*, 17953.
- [7] J. P. Perdew, K. Burke, M. Ernzerhof, *Phys. Rev. Lett.* **1996**, *77*, 3865.